

GTL CA: Mono Co: Long Valley  
KGRA

Magnetic

PAL. 501. L Valley  
Magnetic

Copy - Mono County  
CA 101

A MAGNETIC MODEL STUDY  
OF THE  
LONG VALLEY CALDERA, CALIFORNIA

By

Frederick E. Berkman

A thesis submitted to the Faculty and the Board of Trustees  
of the Colorado School of Mines in partial fulfillment of the require-  
ments for the degree of Master of Science, Geophysics.

Signed: Frederick E. Berkman  
Frederick E. Berkman

Golden, Colorado

Date: December 21, 1978

Approved: George V. Keller  
George V. Keller  
Thesis Advisor and  
Head of Department of  
Geophysics

Golden, Colorado

Date: December 21, 1978

ABSTRACT

The Long Valley caldera lies on the eastern front of the Sierra Nevada batholith about 25 kilometers south of Mono Lake, California. The Long Valley caldera is a 350 km<sup>2</sup> topographic depression which was created 0.7 m.y. ago by the subsidence of a caldron block following a massive eruption. The Bishop Tuff is the major eruptive unit and it forms an extensive rhyolite ash flow outside the caldera. Inside the caldera, the Bishop Tuff is covered by post eruption ejecta, resurgent flows and lake sediments. The volcanic units related to the formation, eruption and resurgence of the caldera are underlain by the batholithic granites which locally contain pendants of meta-volcanic and metasedimentary rocks.

An array of geophysical exploration techniques have been applied in the Long Valley area; gravity, magnetics, seismic refraction profiles, direct current resistivity soundings, and time-domain electromagnetic soundings. The results indicate that two separate basins lie within a well defined ring fracture zone. The eastern and western basins are about 3 and 2 km deep respectively. They are separated by major faults which extend into the central part of the caldera. Bishop Tuff fills the caldron from above the collapse block to within 0.5 to 1.5 km of the ground surface.

A magnetic model of the Long Valley area was constructed from aeromagnetic data and evaluated by comparing it with the other

available geophysical, geological and drilling data. The process consists of assembling the total magnetizations and the location coordinates of a number of polygonal prisms and calculating the magnetic field above the prisms. The parameters are adjusted within the data constraints until the calculated and observed magnetic fields agree.

The final prism parameters reveal that the Bishop Tuff in the western basin has had its total magnetization altered to one-fifth of the total magnetization of the Bishop Tuff in the eastern basin. This alteration is mostly a result of the resurgent episodes in the west basin. The volume of altered tuff ( $135 \text{ km}^3$ ) is about 45 percent of the total volume of intracaldera Bishop Tuff ( $300 \text{ km}^3$ ). Seventy-seven  $\text{km}^3$  of Glass Mountain rhyolite lies below the Bishop Tuff in the northeast part of the caldera. A second precaldera mountain is located beneath the Bishop Tuff in the south central area of the caldera.

The magnetic modelling study supports the results of the other geophysical and geological studies in showing that the western basin of the Long Valley caldera is a likely location for a hot water geothermal system.

TABLE OF CONTENTS

	<u>Page</u>
Abstract -----	iii
Acknowledgments -----	vii
Introduction -----	1
Geologic Setting -----	3
Precaldera Volcanics -----	5
Long Valley Caldera -----	7
Postcaldera Collapse Activity -----	8
Pleistocene Long Valley Lake -----	9
Hydrothermal Manifestations -----	9
Tectonics -----	10
Results of Previous Geophysical Studies -----	11
Gravity -----	11
Magnetics -----	13
Seismic Refraction -----	16
Electrical Resistivity Studies -----	19
Synthesis of the Model -----	23
General Constraints -----	23
Modelling Program -----	24
Rock Magnetic Properties -----	25
Results -----	30
Discussion of the Residual Magnetic Field -----	35
Conclusion -----	40
References cited -----	42

LIST OF FIGURES

<u>Figures</u>	<u>Page</u>
1. Generalized geologic map of the Long Valley - Mono Basin area -----	4
2. Generalized geologic map of Long Valley caldera -----	6
3. Combined geology and complete Bouguer gravity map -----	12
4. Combined geology and low-level magnetic intensity map -----	14
5. High level magnetic intensity map -----	15
6. Map showing locations of refraction shot points and recording units -----	17
7. Cross sections showing P-wave velocity structures under the two refraction profiles -----	18
8. Map showing the location of VES and TMS and resistivity cross section segments -----	20
9. Fence diagram constructed from electrical sounding interpretations -----	21
10. Generalized flow diagram for magnetic modelling computes program -----	26
11. Calculated magnetic intensity map of Long Valley -----	37
12. Digitized high-level magnetic intensity map of Long Valley --	38
13. Residual magnetic intensity map of Long Valley -----	39

TABLE

1. Comparison of Rock Magnetizations -----	28
--	----

## ACKNOWLEDGMENTS

The U.S. Geological Survey gave me the opportunity to work on this project. I am indebted and grateful to Dr. David Williams who was always there to discuss the problems.

I wish to thank my thesis advisor, Dr. G.V. Keller for his continuing encouragement. Dr. Norman Harthill generously gave me suggestions for improving the writing. Last, but not least, I am very grateful to Marge Carey for her excellent typing.

## INTRODUCTION

The Long Valley caldera, a volcanic collapse structure in east central California (Figure 1), has been the subject of numerous geologic and geophysical studies and some drilling tests. Many of these investigations are a consequence of the decision of the United States Geological Survey that it would be the test area for hot water geothermal systems; only the Yellowstone caldera in the western United States is known to be younger. Gilbert (1938) first recognized Long Valley as the most likely source area for the Bishop Tuff and suggested that the valley resulted from its eruption. Potassium-argon dating (Dalrymple and others, 1965) indicated that the eruption of the Bishop Tuff occurred about 0.7 m.y. ago. Based on geologic maps by Rinehart and Ross (1957, 1964) and Huber and Rinehart (1965), Smith and Bailey (1968) stated that the Long Valley caldera was resurgent. Bailey and others (1976) summarized the sequence of pre-eruptive and resurgent events and state that the intracaldera hydrothermal activity began at least 0.3 m.y. ago.

The primary purpose of this study is to use aeromagnetic data to refine previous interpretations about the shape and volume of the volcanic units which surround and partly fill the caldera. A secondary purpose is to locate areas of reduced magnetization caused by hydrothermal alteration. First, a summary of the geologic setting of the Long Valley area is presented. Second, the results of the pertinent

geophysical work are described. Third, the synthesis of the magnetic model is explained. Fourth, the results of the final model are discussed and interpreted. Fifth, the conclusions arrived at in the present survey are presented.

### GEOLOGIC SETTING

Long Valley is located in east central California midway between Mono Lake and Bishop, immediately east of the Sierra Nevada Mountains (Figure 1). It is an elliptical topographic depression with an area of about 450 km<sup>2</sup> surrounded by mountains except to the southeast. Elevations within the caldera range from 2067 m (6,781 feet) at Lake Crowley to 4010 m (13,163 feet) at Red Mountain, 13 km southwest of Lake Crowley.

The region east of the eastern boundary of the Sierra Nevada is a structurally depressed area which may be divided into a northern part and a southern part, based on topography and geologic history. Long Valley lies in the boundary zone between the northern and southern parts where the volume and variety of late Cenozoic volcanism has been unusually large (Gilbert, 1968).

The oldest rocks in the area of investigation are the Mount Morrison and Ritter Range roof pendants. The metasediments of the Ritter Range pendant are lithologically similar to, and correlate with, the metasediments of the Mount Morrison pendant (Huber and Rinehart, 1965). The Mount Morrison pendant is exposed to the south of the caldera's ring fracture zone. The Ritter Range pendant is west of the caldera. These pendants both lie within the Sierra Nevada batholith and are remnants of Ordovician, Pennsylvanian and Permian sediments and Jurassic volcanics, which were mechanically and thermally metamorphosed during the emplacement of the batholith in the Jurassic and

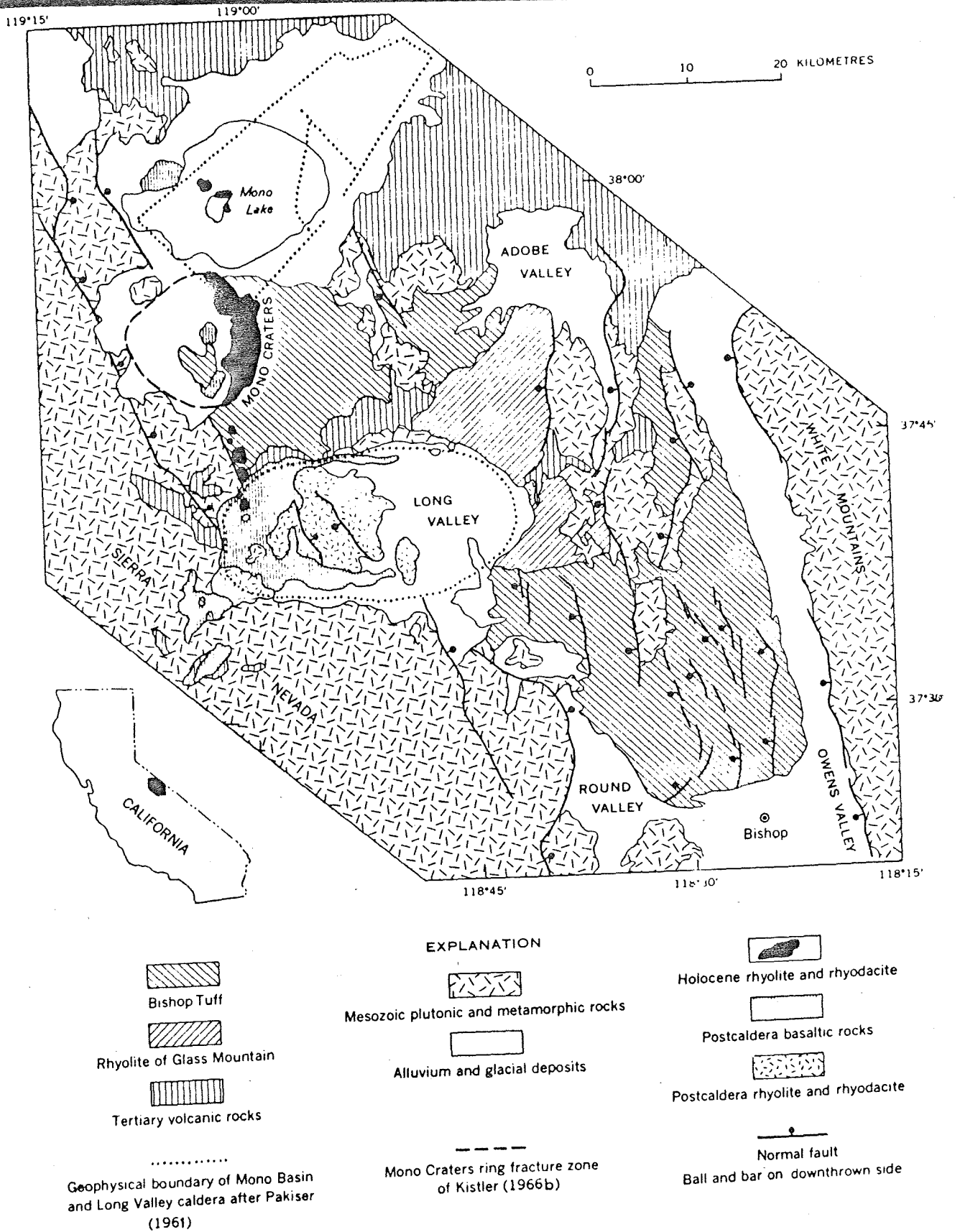


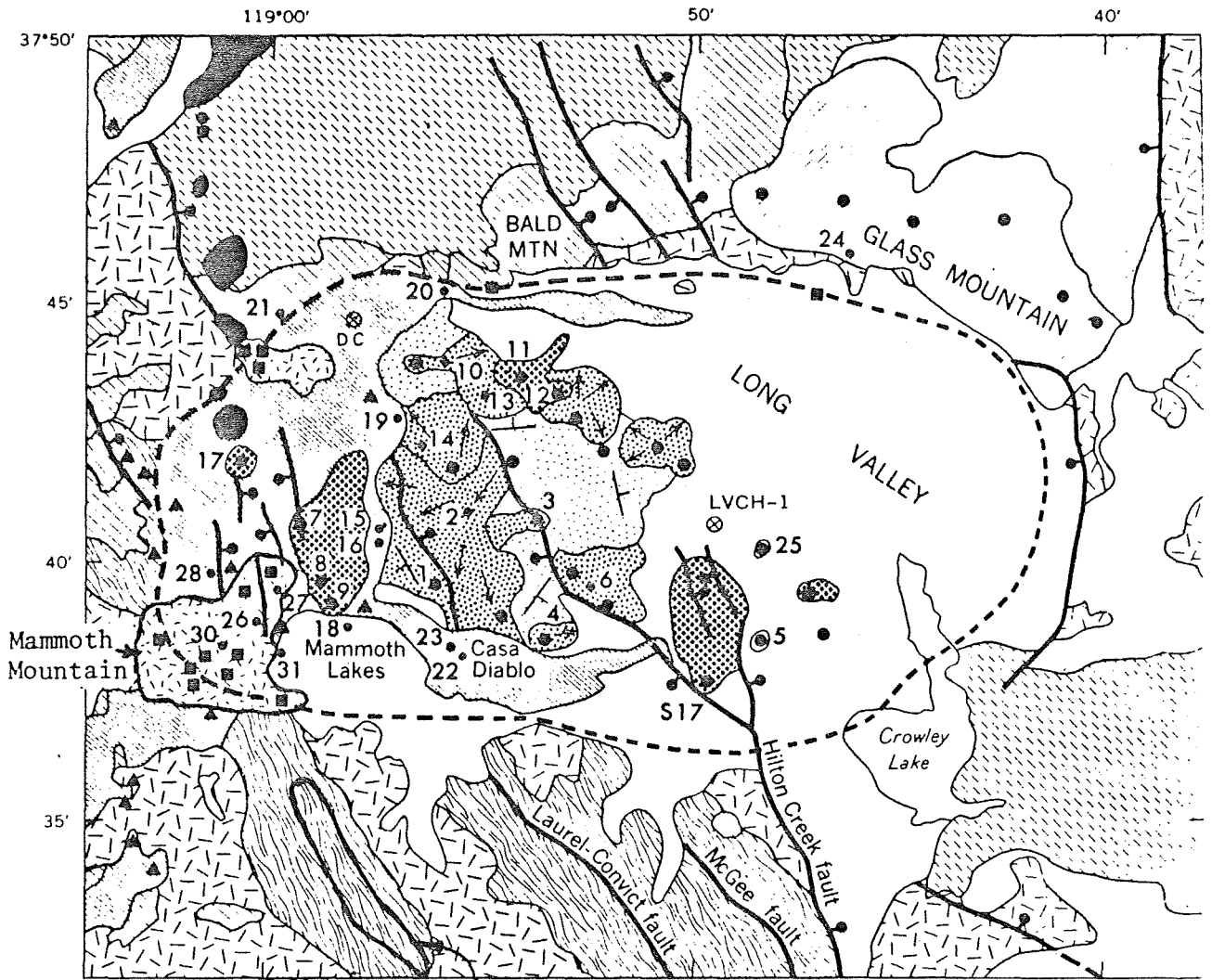
Figure 1. Generalized geologic map of the Long Valley-Mono Basin area from Bailey and others, 1976.

Cretaceous periods. The Jurassic-Cretaceous geosynclinal rocks were intruded by the granitic rocks of the batholith. After uplift during the Tertiary, the mountains were repeatedly glaciated and eroded (Bateman and others, 1963).

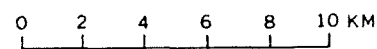
#### Precaldera Volcanics

Tertiary volcanic rocks, mostly basalt, andesite and rhyodacite overlie the basement rocks. An erosional surface of moderate relief exists between the basement rocks and the Tertiary volcanic rocks (Bailey and others, 1976). The main mass of San Joaquin Mountain and Two Teats is composed of rhyodacites overlying basalts (Figure 2). These two mountains just northwest of the caldera erosional remnants of a large Pliocene volcano. Along the north rim of the caldera are three more exposures of rhyodacite, the largest exposure is known as Bald Mountain. Minor andesite and basalt flows occur on the east and south caldera rim (Bailey and others, 1976). Potassium-argon ages for these Tertiary volcanic rocks range from 3.2 to 2.6 m.y. old (Dalrymple, 1963).

The Glass Mountain rhyolites are the oldest volcanic rocks that can be related to the Long Valley magma chamber (Bailey and others, 1976). Glass Mountain and its neighboring peaks are a thick (>1 km) mantle of ash falls covering contemporaneous flows, domes and epiclastic sediments (Rinehart and Ross, 1957). The exposed vents and intrusive centers form an arc subparallel to the northeast caldera wall. They possibly represent early magma chamber leakage which was controlled by initial ring fracturing. From Glass Mountain, dissected flanking flows extend to the northeast, south and most probably into Long



Quartz latite tuff  
of Skeldon Lake



E X P L A N A T I O N

- |  |   |  |  |
|--|---|--|--|
|  | Alluvium, glacial deposits, and caldera fill                          |  | rhyolite                                       |
|  | Holocene rhyolite-rhyodacite  |  | rhyodacite                                     |
|  | Late basaltic rocks   |  | basalt andesite                                |
|  | Rim rhyodacites   |  | K-Ar sample locality                           |
|  | Moat rhyolites  |  | Drill hole                                     |
|  | Early rhyolites { tuffs: fine dotted<br>flows: coarse dotted          |  | Direction of dip of strata                     |
|  |   |  | General direction of flowage of lava           |
|  | Bishop Tuff   |  | Normal fault - ball and bar on downthrown side |
|  | Rhyolite of Glass Mtn { dome flows: fine lined<br>tuffs: coarse lined |  | Outline of Long Valley caldera floor           |
|  |   |  |  |
|  | Tertiary volcanic rocks   |  |  |
|  | Jurassic-Cretaceous granitic rocks                                    |  |  |
|  | Paleozoic-Mesozoic metamorphic rocks                                  |  |  |

Figure 2. Generalized geologic map of Long Valley caldera from Bailey

Valley where they are down-faulted and covered by the intracaldera Bishop Tuff and lake sediments (Bailey and others, 1976). Potassium-argon age determinations from Obsidian sampled near the top of Glass Mountain are about  $0.90 \pm 0.10$  m.y. before present (bp). The age of biotite rhyolite sampled at the southwest base of the mountain is  $1.92 \pm 0.05$  m.y. bp (Gilbert and others, 1968). These ages indicate Glass Mountain was created by eruptions extending over a 1 m.y. time span.

#### Long Valley Caldera

The Bishop Tuff explosively erupted about 0.7 m.y. bp (Dalrymple, et al., 1965) from vents (Gilbert, 1938), now covered by ejecta, resurgent flows and lake sediments. The explosion was sufficiently violent and voluminous to deposit Bishop ash beds in eastern Nebraska (Izett and others, 1965). The Bishop Tuff is exposed outside the caldera as an extensive rhyolite ash flow sheet. It is mostly composed of glass shards but contains as much as 30 percent phenocrysts of quartz-sanidine, plagioclase, biotite, Fe-Ti oxides and contains grains of iron oxide scattered through the tuff matrix (Gilbert, 1938). Bishop Tuff is not exposed in the caldera but its presence at depth is indicated by inclusions in exposed post-caldera rhyolite tuffs (Bailey, 1973). During, or shortly after the eruption of the Bishop Tuff, the roof of the magma chamber collapsed. The surface area of the subsided block calculated from the position of the main boundary faults is  $350 \text{ km}^2$ . Bailey and others (1976) used this area and a thickness of 1 km to estimate a volume of  $350 \text{ km}^3$  for the erupted Bishop Tuff.

### Postcaldera Collapse

More eruptions followed the subsidence and a dome formed in the west central part of the collapsed caldera. Ages of 0.73 to 0.63 m.y. have been measured for these early rhyolites which are exposed in the vicinity of the central caldera (Bailey and others, 1976). Bailey and others (1976) mapped 12 eruptive vents for the early rhyolites, many of which are aligned along northwest trending faults. The resurgent dome (Smith and Bailey, 1968) is composed of faulted blocks and was an island in the caldera lake. Rhyolites continued to erupt after doming; three groups of eruptions occurred approximately 0.5, 0.3 and 0.1 m.y.b.p. from vents in the moat around the flanks of the resurgent dome. The location of the moat rhyolites is probably related to the ring fractures surrounding the resurgent dome and frontal faults along the Sierra Nevada. Their 0.2 m.y. long cycle may reflect pressure buildup and release in the magma chamber (Bailey and others, 1976). Hornblendebiotite rhyodacites erupted along the outer rim 0.2 to 0.05 m.y.b.p., Mammoth Mountain, a volcano on the southwest rim of the caldera, is the largest of these rhyodacite eruptions. Rhyodacite domes also occur on the northwest rim along Deadman Creek and on the north rim near Bald Mountain and Glass Mountain. Several basalt flows in the western moat occurred contemporaneously with the moat rhyolite and rim rhyodacite eruptions (Bailey and others, 1976). The Inyo craters and domes are the most recent volcanic structures in the caldera. Their ages range from about 720 to 650 years (Rinehart and Huber, 1965).

### Pleistocene Long Valley Lake

Immediately after caldera subsidence, the depression began to fill with water which formed a moat around the resurgent dome. Over a time period of about 0.60 m.y., the lake water cut through the Bishop Tuff along the southeast caldera rim forming the ancestral Owens River until the downcutting completely drained the lake. Holes drilled by the U.S.G.S. indicate that the lake deposits are at least 305 m thick (Bailey and others, 1976).

### Hydrothermal Manifestations

Fossil gas vents, ancient sinter deposits and acid alteration indicate that hydrothermal activity in Long Valley was more intense than similar activity in the Yellowstone caldera today. Silicification, argillization and zeolitization processes have sealed fractures and reduced porosity to a depth of least 300 m. The intensity and distribution of these sealing processes are closely related to temperature and ground water levels. Most of the currently active hot springs and fumeroles are on or near extensions of the Hilton Creek fault into the caldera (Figure 2), indicating that the sealing material is fractured along the currently active faults. The location of most of the hydrothermal activity outside and around the resurgent dome indicate that it may be controlled by the caldera ring fracture (Bailey and others, 1976).

### Tectonics

During the million year period that the Long Valley magma chamber sustained volcanism, the Sierra Nevada mountain range was undergoing uplift. The rise of the Sierra Nevada was nearly complete before the Pleistocene glaciation. The eastern Sierra Nevada escarpment resulted from down-faulting along the eastern portion of the front during the last 3 m.y. (Bateman and Wahrhaftig, 1966; Christensen, 1966). The Long Valley magma chamber is located across major faults of the Sierra Nevada system. The Hartley Springs fault intersects the northeast wall of the caldera. The Hilton Creek fault intersects the southeast caldera rim (Figure 2). Both these faults split into many minor faults inside the caldera. Bailey and others (1976) feel that as the magma chamber solidified, the down-faulting along these frontal faults was directed through the western part of the caldera instead of around the ring fracture system. Bailey and others also feel that the style of faulting indicates that the structural block containing the caldera is not as rigid as the surrounding crust and may still be underlain by magma.

RESULTS OF PREVIOUS GEOPHYSICAL STUDIES

Many geophysical techniques have been applied in the Long Valley area. They provided the quantitative information needed to devise a detailed magnetic model. The following section contains a short summary of results from gravity, magnetic, seismic refraction, direct current resistivity and time-domain electromagnetic exploration techniques.

Gravity

Based on early gravity data, Pakiser and others (1961, 1964) concluded that Long Valley is a steep-sided structural basin filled to a depth of about 12,000 feet with Cenozoic volcano-clastic rock. Kane and others (1976) used additional gravity stations to refine Pakiser's interpretations. Both the porous caldera fill and the magma chamber beneath the fill could be expected to produce gravity lows. The principal gravity low coincident with Long Valley has a magnitude of about 50 mgal; the complete Bouguer gravity map based on about 500 stations is shown in Figure 3. The caldera boundary is marked by steep gravity gradients which flatten inside the caldera; outside the caldera, the east-west elliptical structure is lost. Kane and others (1976) produced a model of the caldera fill from the residual gravity using an average density contrast of  $0.45 \text{ g/cm}^3$ . Two major sources of error in this inversion process come from the selection of the regional surface and density variation in the fill. The model of the caldera fill of Kane and others (1976) shows two basins separated by a high central platform. The eastern basin is estimated to be 3 km deep and the western basin is about 2 km deep. These depths agree well with

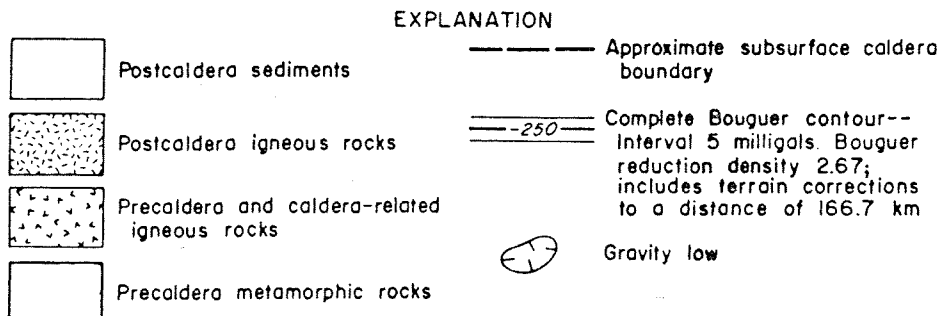
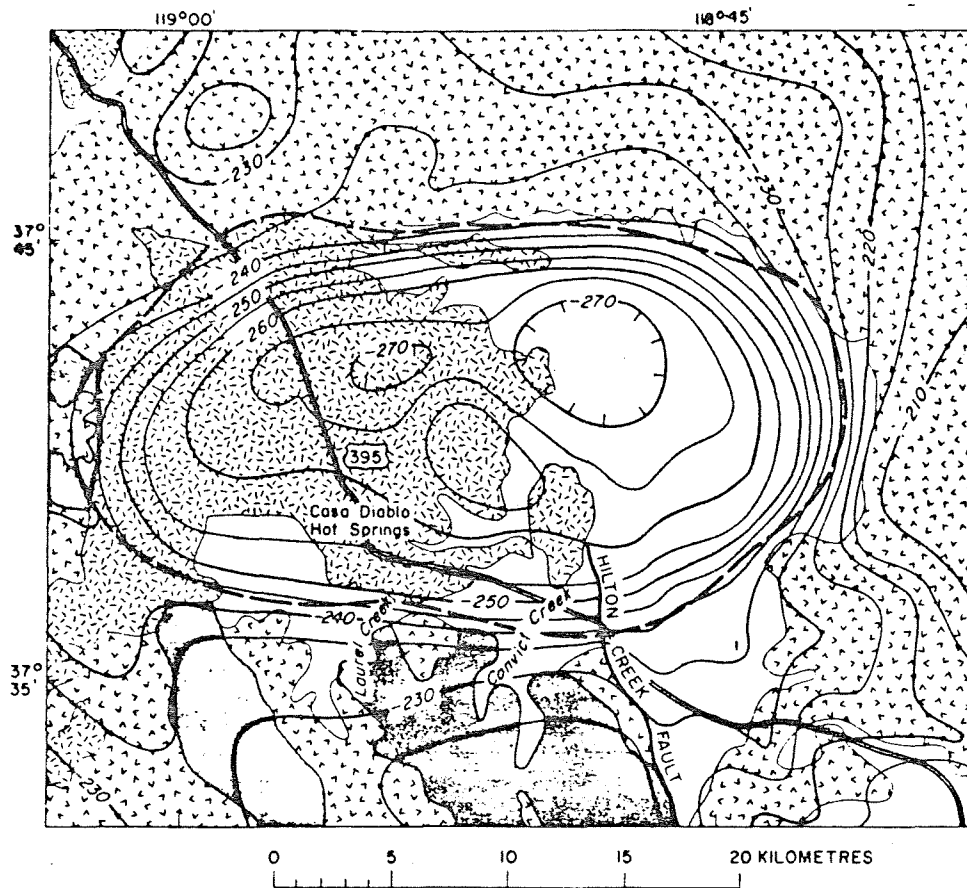


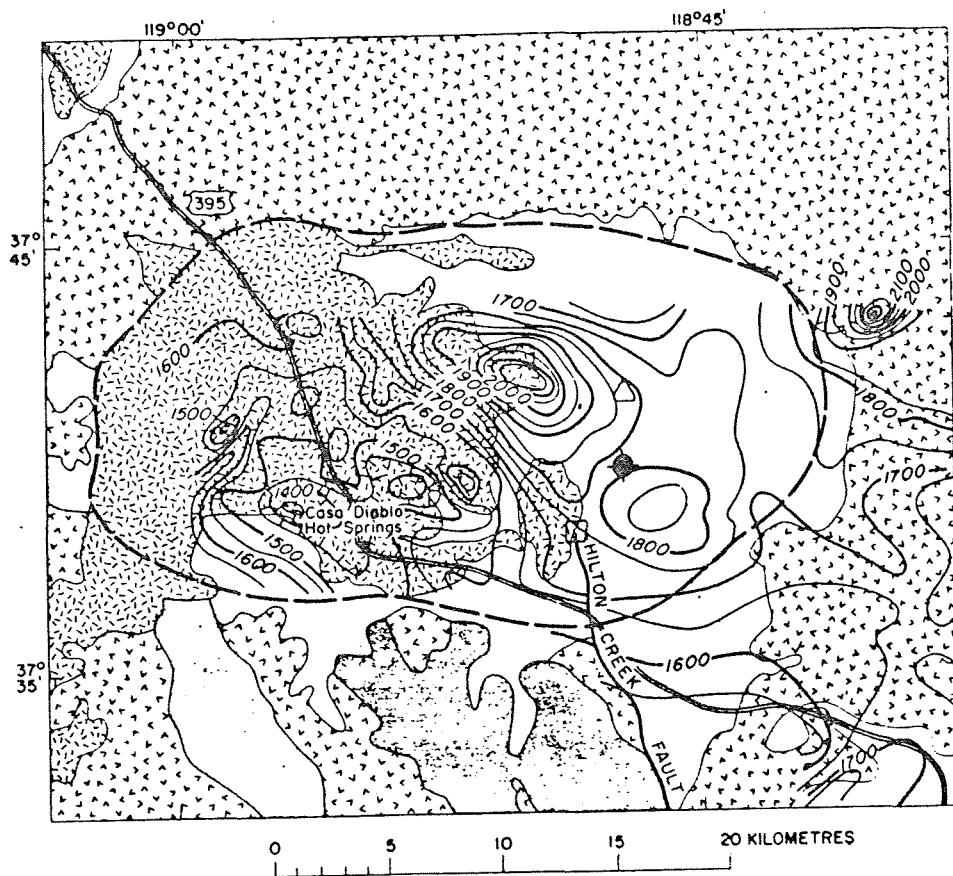
Figure 3. Combined geology and complete Bouguer gravity map of Long Valley caldera from Kane and others, 1976.

those from the seismic refraction work of Hill (1976). Within the area surveyed, Kane and others (1976) could not conclusively isolate the gentle gravity gradients produced by a deep magma chamber.

### Magnetics

A low altitude aeromagnetic survey was flown over most of the caldera in 1963 at an altitude of 2,660 m (9,500 feet) above sea level. The topographic elevations vary from 2,067 m (6,781 feet) at Lake Crowley to 2,626 m (8,615 feet) on top of the resurgent dome in the western caldera. East-west flight lines were spaced 1 to 1.5 km apart (Henderson and others, 1963). No regional trends were removed from the total magnetic intensity map (Figure 4). A second survey was flown during 1973 at an altitude of 4 km (13,500 feet) above sea level (U.S.G.S. O.F. 1974). This survey had flight lines 1.7 km apart and a regional trend was removed using the 1965 International Geomagnetic Reference Field (I.G.R.F.) corrected for secular variations to 1973 (Cain and others, 1967), (Figure 5).

The two aeromagnetic surveys show a double-peaked magnetic high which trends northwest to southeast over the eastern half of the caldera. Kane and others (1976) interpreted the double magnetic highs to be volcanic necks that were sources of flows which produced the elongated magnetic high over the eastern caldera (Figures 4 and 5). This interpretation is to be preferred rather than a local susceptibility change because it best fits the gravity data. Both surveys show a large magnetic low surrounding Casa Diablo Hot Springs (Figure 4). On the lower survey, this magnetic low is composed of several separate closed magnetic lows. The higher survey shows the Casa



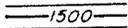
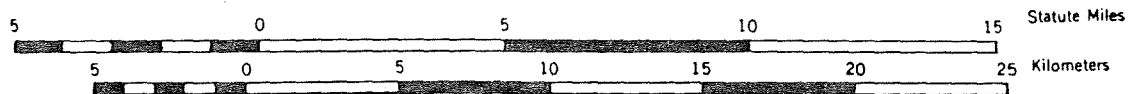
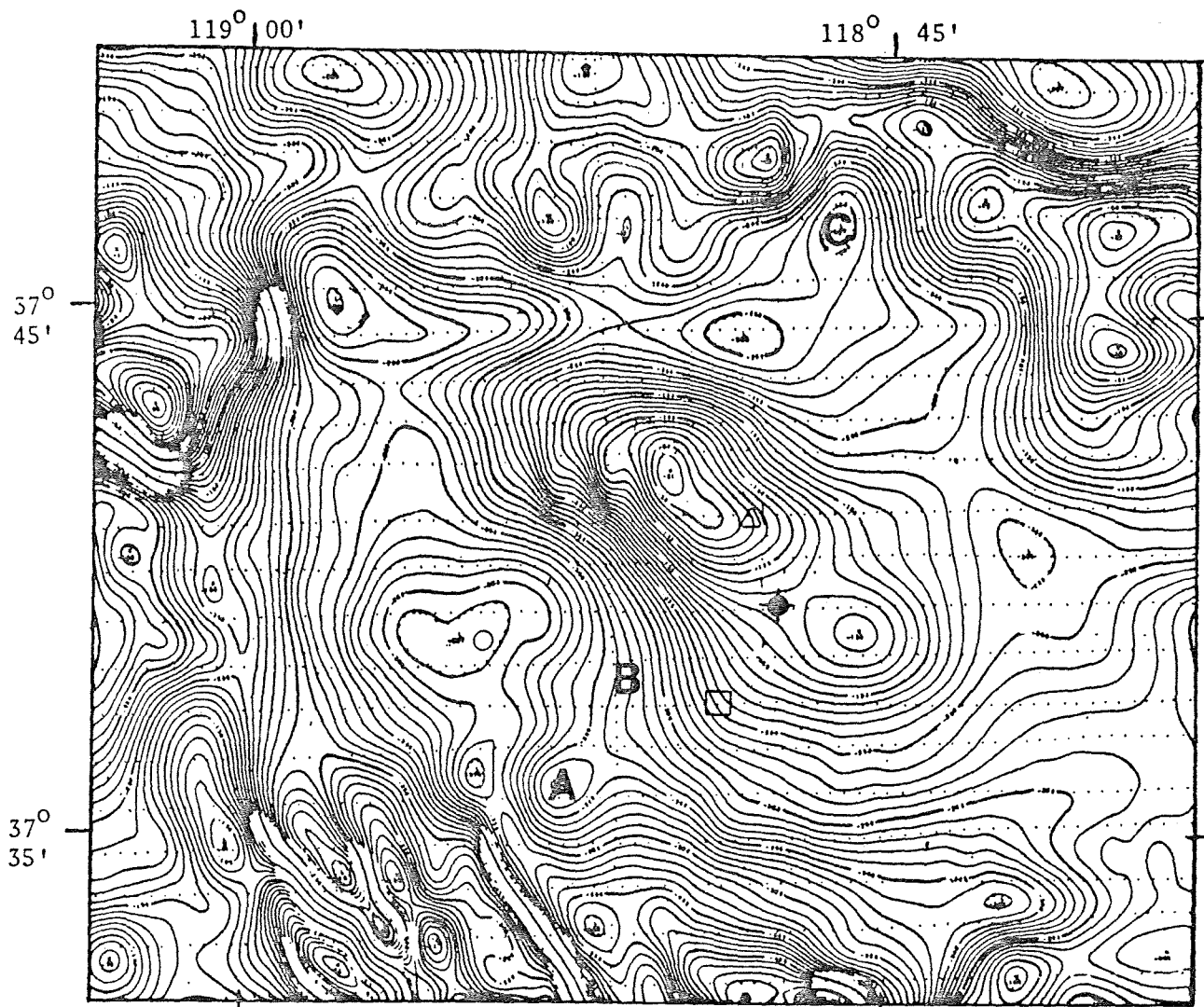
- EXPLANATION
- |   |  |  |   |
|---|--|--|---|
|  | Postcaldera sediments                        |  | Approximate subsurface caldera boundary   |
|  | Postcaldera igneous rocks                    |  | Total intensity magnetic contour--Contoured with respect to an arbitrary datum. Interval 50 gammas. Flown at 9,000-foot barometric altitude |
|  | Precaldera and caldera-related igneous rocks |  | Magnetic low  |
|  | Precaldera metamorphic rocks                 |  |   |
|  | Cashbaugh Ranch                              |  |   |
|  | Whitmore Hot Springs                         |  |   |
|  | Republic Geothermal Well                     |  |   |

Figure 4. Combined geology and low level magnetic intensity map of Long Valley caldera from Kane and others, 1976.



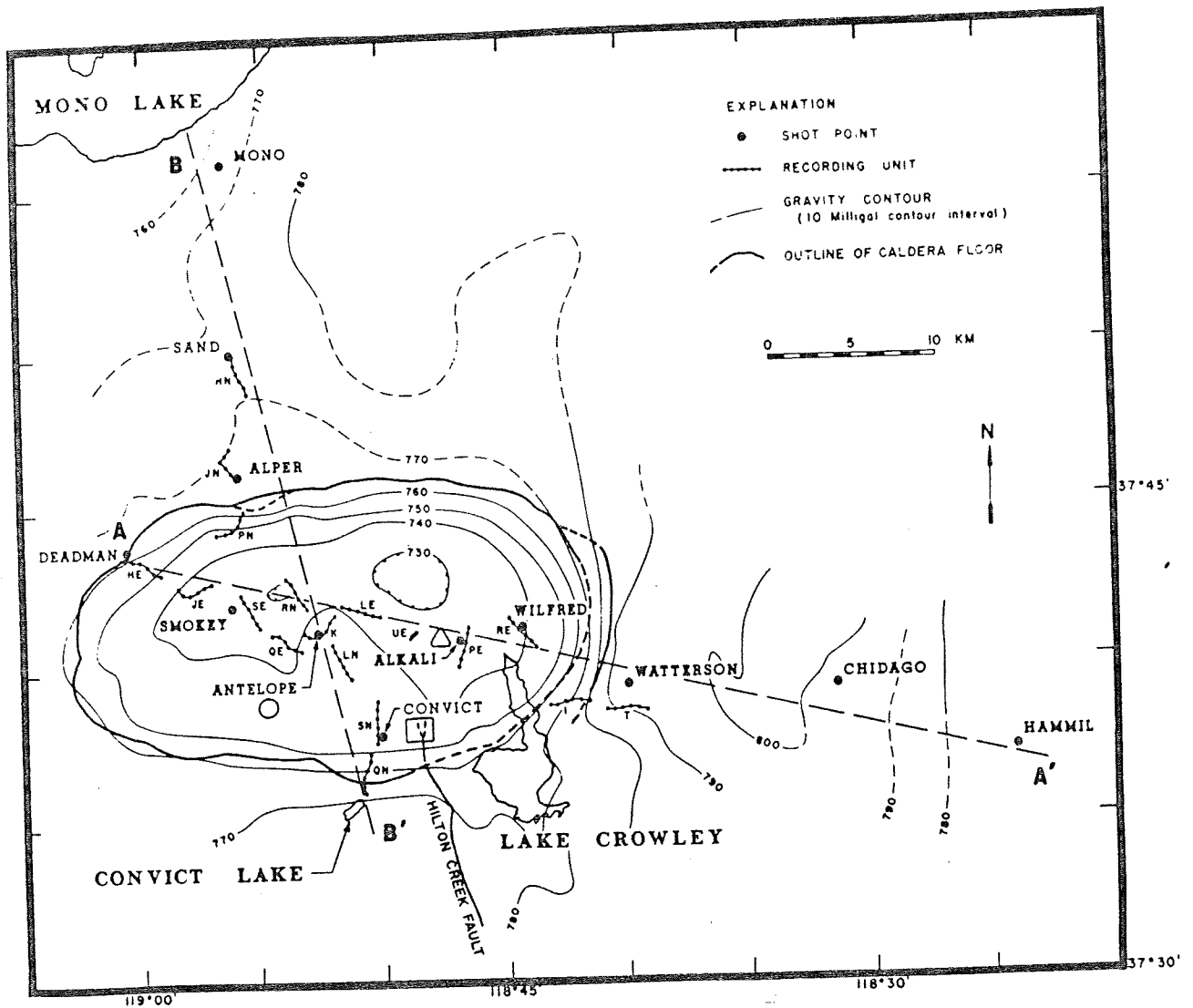
- ..... Flight Lines                      Contour interval 10 gammas
- A** Small closed magnetic high over outcrop of Round Valley Peak granodiorite
  - B** Location of buried precaldera mountain composed of Round Valley Peak granodiorite
  - C** -257 gamma low over volcanic vent on flank of Glass Mountain
  - Casa Diablo Hot Springs
  - Whitmore Hot Springs
  - △ Cashbaugh Ranch
  - ◆ Republic Geothermal Well

Figure 5. High level magnetic intensity map of Long Valley and vicinity

Diablo low as part of a regional magnetic low extending north-south through the western part of the caldera. The source of the Casa Diablo magnetic low is interpreted to be rock which has had its magnetite content altered by hydrothermal solutions (Kane and others, 1976). They also interpret the source of the larger magnetic low as a belt of metasedimentary rocks extending beneath the western caldera floor.

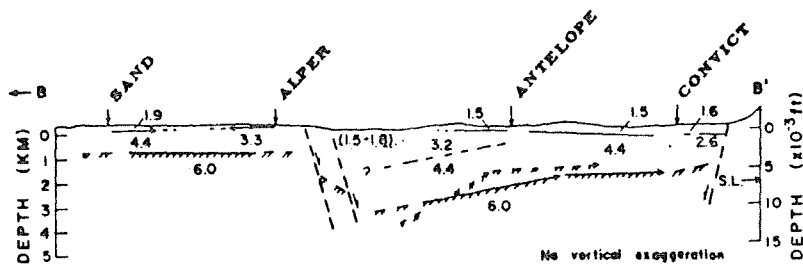
#### Seismic Refraction

Two intersecting seismic refraction lines were shot across the caldera by Hill (1976), (Figure 6). Four P-wave velocities were picked from the time vs. distance plots. Hill estimates that the P-wave velocities are correct to within  $\pm 10$  percent and the interface depths are correct to within  $\pm 20$  percent. The east-west velocity depth profile of Hill (1976), (Figure 7) is quite similar to Bailey's (1976) east-west geologic cross-section through the caldera. On the basis of this similarity, the following associations were made: The granitic and metamorphic basement rocks have a P-wave velocity of  $6.0 \pm 0.4$  km/sec, the Bishop Tuff and Glass Mountain rhyolite have a P-wave velocity of 4.0 to 4.4 km/sec, post-collapse rhyolite, rhyodacite and basalts have a velocity of 2.6 to 3.4 km/sec, the weathered layer velocity is 1.5 to 1.9 km/sec. Hill (1976) makes several major conclusions: The basement rocks in the caldera have been down-dropped 2.5 to 3 km along the north and northwest sides of the caldera and 1 to 2 km along the south and east sides, there is a step-like displacement in the basement along the northward

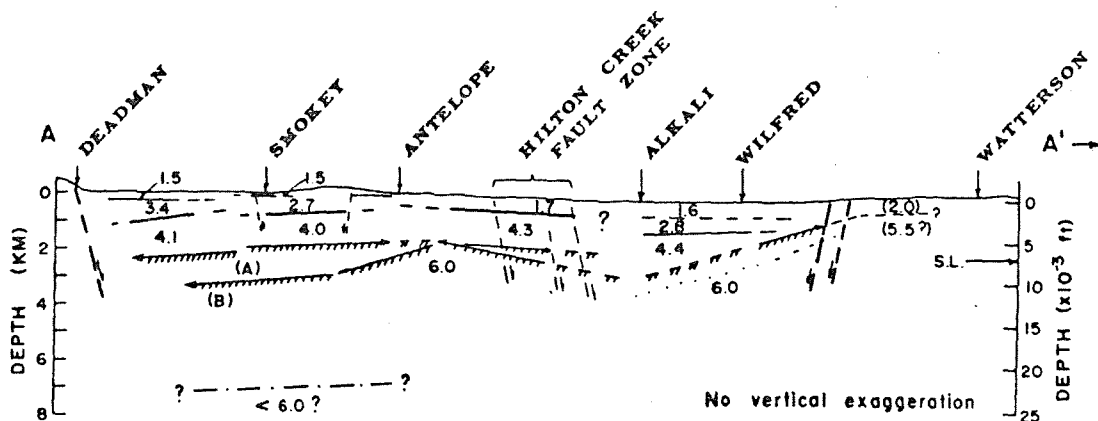


- △ Cashbaugh Ranch
- Whitmore Hot Springs
- Casa Diablo Hot Springs

Figure 6. Map showing locations of shot points and recording units with respect to the outline of the caldera floor and 10 mgal. gravity contours from Hill, 1976.



Cross section showing P wave velocity structure under profile BB'. Symbols are explained below.



Cross section showing P wave velocity structure under profile AA'. Numbers are P wave velocities in kilometers per second. Depths are with respect to average surface elevation (2.1 km); S.L. indicates sea level. Heavy lines indicate horizons with reversed subsurface coverage. Light lines indicate horizons with one-way subsurface coverage; arrows indicate propagation direction of subsurface waves along the horizon. Dashed lines indicate horizons based on later arrivals or extrapolated horizons. Basement horizon is indicated by hachures. Faults are indicated by steeply dipping dashed lines with arrows showing sense of displacement (Hill, 1976).

Figure 7.

extension of the Hilton Creek fault into the caldera, the top of the Bishop Tuff layer is domed in the vicinity of the resurgence features and has a maximum relief of  $\frac{1}{2}$  to 1 km.

### Electrical Resistivity Studies

A total field resistivity map was compiled from measurements made inside the caldera ring fracture zone (Figure 8, Stanley and others, 1976). The dipole measurements were located around four long (3 to 5 km) bipole current sources. Direct current vertical electrical soundings (VES) using the Schlumberger array were made by Stanley and others (1976) as were time-domain electromagnetic soundings (TDEM).

The results of the electrical surveys indicate the existence of two major zones of low resistivity. The resistivity low centered about the Cashbaugh Ranch is characterized by values as low as 2 ohm-m. Stanley and others (1976) stated that the lowest resistivities were measured in a small graben and seem to indicate hot water in the highly fractured rocks of the graben. The second resistivity low has values of less than 40 ohm-m and is centered just south of Casa Diablo Hot Springs. Stanley and others (1976) feel that the central part of the Casa Diablo resistivity low is probably caused by extensive alteration in the tuff unit, hot fluids or both.

Resistivity cross-sections were constructed by Stanley and others (1976) from the vertical electrical soundings and the time-domain electromagnetic soundings (Figure 9). The 1-to-10 ohm-m layer, the lower resistivities found in the survey, represents hydrothermally altered rhyolitic tuffs. The Cashbaugh resistivity low does not

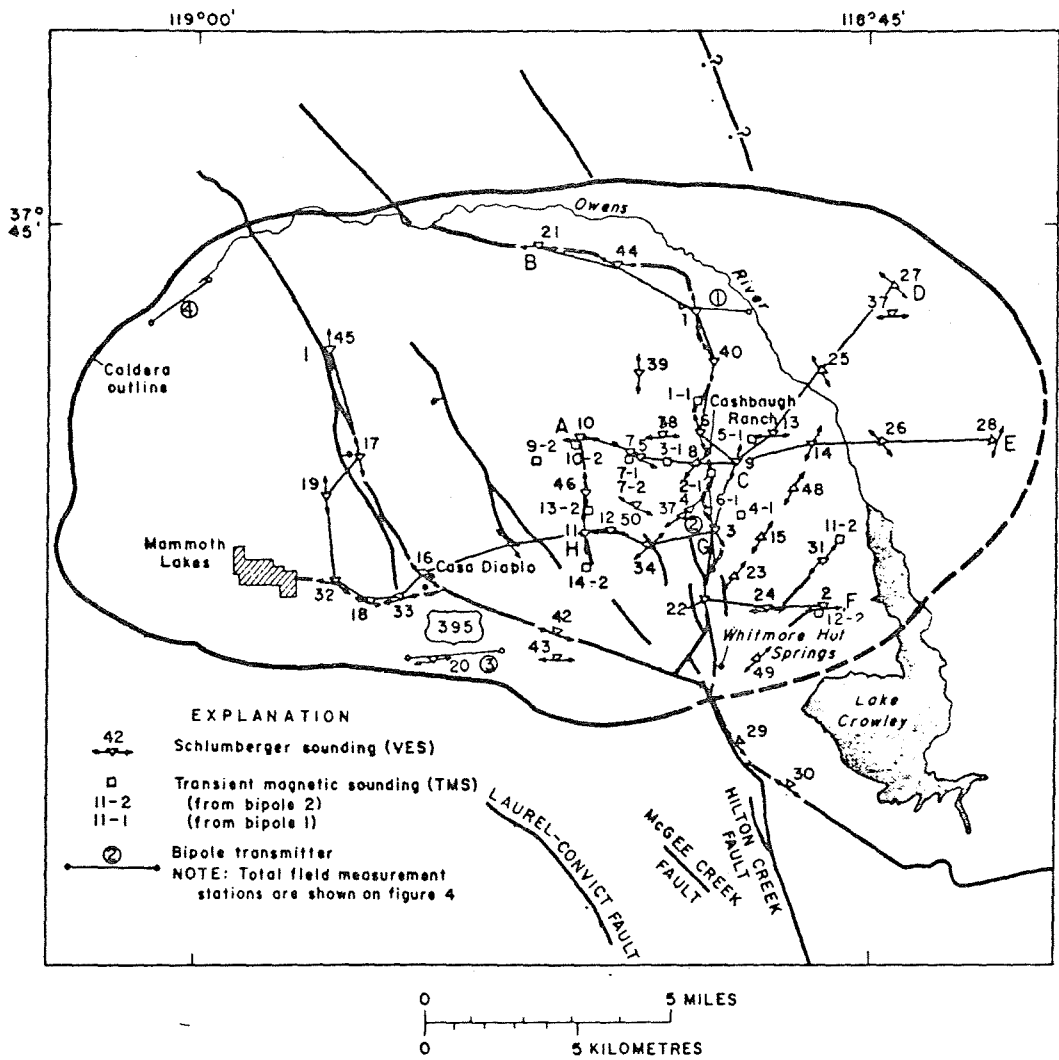


Figure 8. Map showing location of VES and TMS and resistivity cross-section segments used to construct fence diagrams of Figure 9 from Stanley and others, 1976.

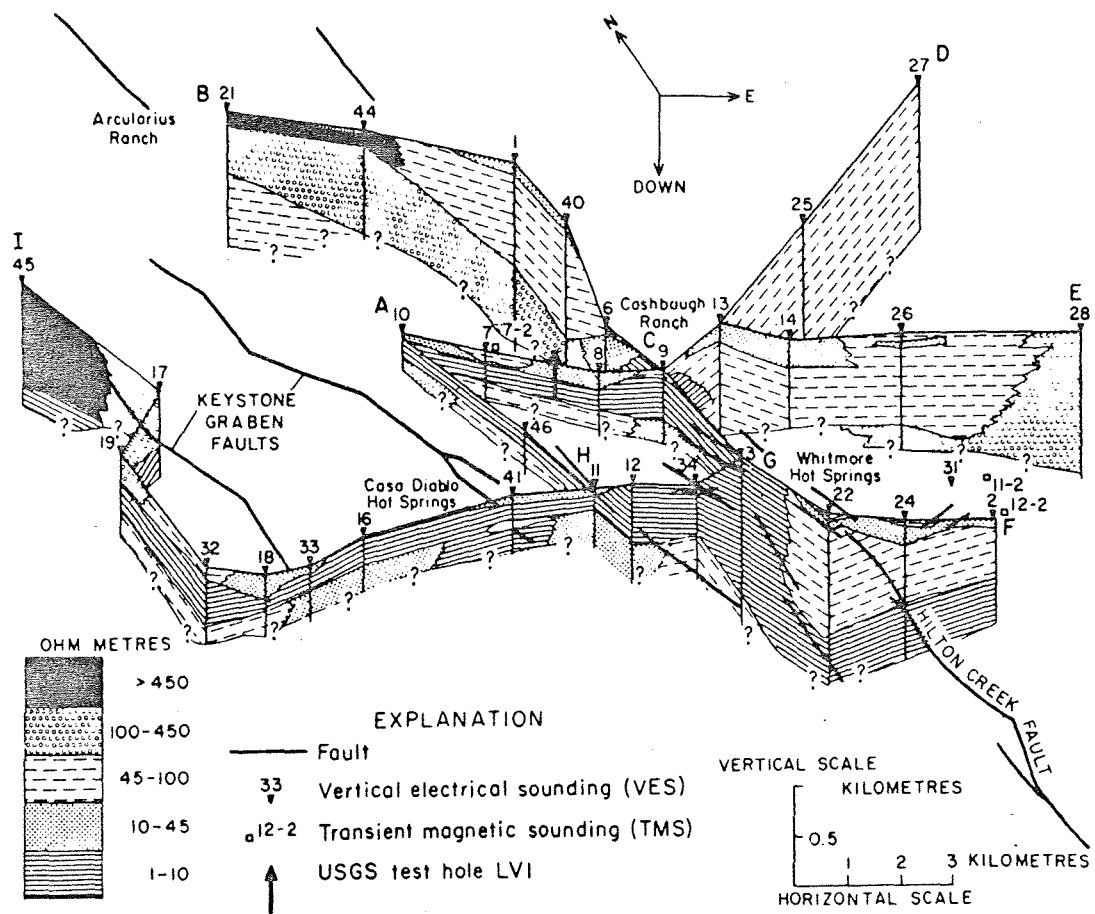


Figure 9. Fence diagram constructed from electrical sounding interpretations from Stanley and others, 1976.

persist below 0.5 km on the fence diagram by Stanley and others (1976), nor does the Casa Diablo Hot Springs resistivity low. However, the Cashbaugh resistivity low does connect laterally with a deep conductor (greater than 0.5 km thick and less than 10 ohm-m resistivity) about 1.2 km below Whitmore Hot Springs. Stanley and others (1976) feel that their resistivity results indicate that the major part of the past hydrothermal activity is controlled by faulting related to the regional displacements along the eastern front of the Sierra Nevada.

### SYNTHESIS OF THE MODEL

Model as used here means the assemblage of prisms which form the shapes of the various distinct magnetic bodies in and around the caldera. The construction of a complicated magnetic model requires an abundance of constraints. Without constraints, magnetic field data do not yield unique values for the location coordinates and total magnetization of the body. Fortunately, these parameters can be determined several ways. Some of the initial locations, dimensions and magnetizations are given in the investigations referred to previously. Often, either size and shape or the total magnetization is unknown. The unknown quantities are determined by comparing the calculated and observed magnetic fields and adjusting the unknowns until the magnetic fields are considered to be in sufficient agreement. The modelling process consists of two basic procedures which are repeated each time new prisms are added. First, the initial parameters for the new prisms are determined. Second, the parameters for all prisms are refined until the calculated magnetic field matches the observed field.

#### General Constraints

Several general constraints are rigidly applied to the modelling process. First, the intensity of total magnetization assigned to each rock type is within a range which would be expected from measured susceptibilities and remanent magnetizations for that rock type. The choice of some ranges is subjective. Second, all the caldera fill material has a positive magnetic polarity. Grommé sampled all the rock types exposed in the area of the resurgent dome and found none

with reversed polarity (personal communication). Also, the caldera collapse and resurgence post-dates the last major reversal of the earth's magnetic field. Third, the direction of magnetization for each prism representing caldera fill is coincident with the direction of the earth's present magnetic field in Long Valley. The volcanic rocks in the fill are young and probably have not been rotated from their original position, (Grommé, personal communication). Fourth, the bottom of the model is 1.25 km (4,240 feet) below sea level. This depth is chosen because it is the bottom of the deepest Bishop Tuff accumulation in the caldera and it is well defined by the refraction survey. Fifth, the size and location of each prism was kept within limits imposed by geological, drilling, and other geophysical data.

#### Modelling Program

The computer program used in this study calculates the exact magnetic fields of right polygonal prisms; demagnetization is neglected. Talwani (1965) suggested a method to calculate the three orthogonal components of a magnetic anomaly, which may be described as:

$$X = J_x V_1 + J_y V_2 + J_z V_3$$

$$Y = J_x V_2 + J_y V_4 + J_z V_5$$

$$Z = J_x V_3 + J_y V_5 + J_z V_6$$

where

X = component of the magnetic field in the x-direction of a Cartesian coordinate system,

- $Y$  = component of the magnetic field in the y-direction,  
 $Z$  = component of the magnetic field in the z-direction,  
 $J_x$  = volume intensity of magnetization in the x-direction,  
 $J_y$  = volume intensity of magnetization in the y-direction,  
 $J_z$  = volume intensity of magnetization in the z-direction,  
 $V_{1-6}$  = volume integrals defined by Talwani (1965, eq. 3).

Talwani evaluated these integrals in closed form except along the z-axes where he applied a minimum-error numerical integration. Plouff (1976) was able to derive an exact expression for the integral along the z-axis. The program used in this study is basically identical to one published by Plouff (1975). A flow diagram of operations for the computer program is given in Figure 10.

### Rock Magnetic Properties

Magnetic susceptibility and remanent magnetization are the physical properties associated with local magnetic anomalies in the earth's magnetic field. These properties are merely assumed to be uniform within the volume of each magnetic body. The total magnetization of a body is the vector sum of the remanent magnetization and the induced magnetization. This can be expressed as:

$$\vec{J} = kH\vec{r} + J_{NRM} \vec{r}$$

where

$k$  = magnetic susceptibility

$H$  = intensity of earth's inducing field in the direction of the unit vector  $\vec{r}$ .

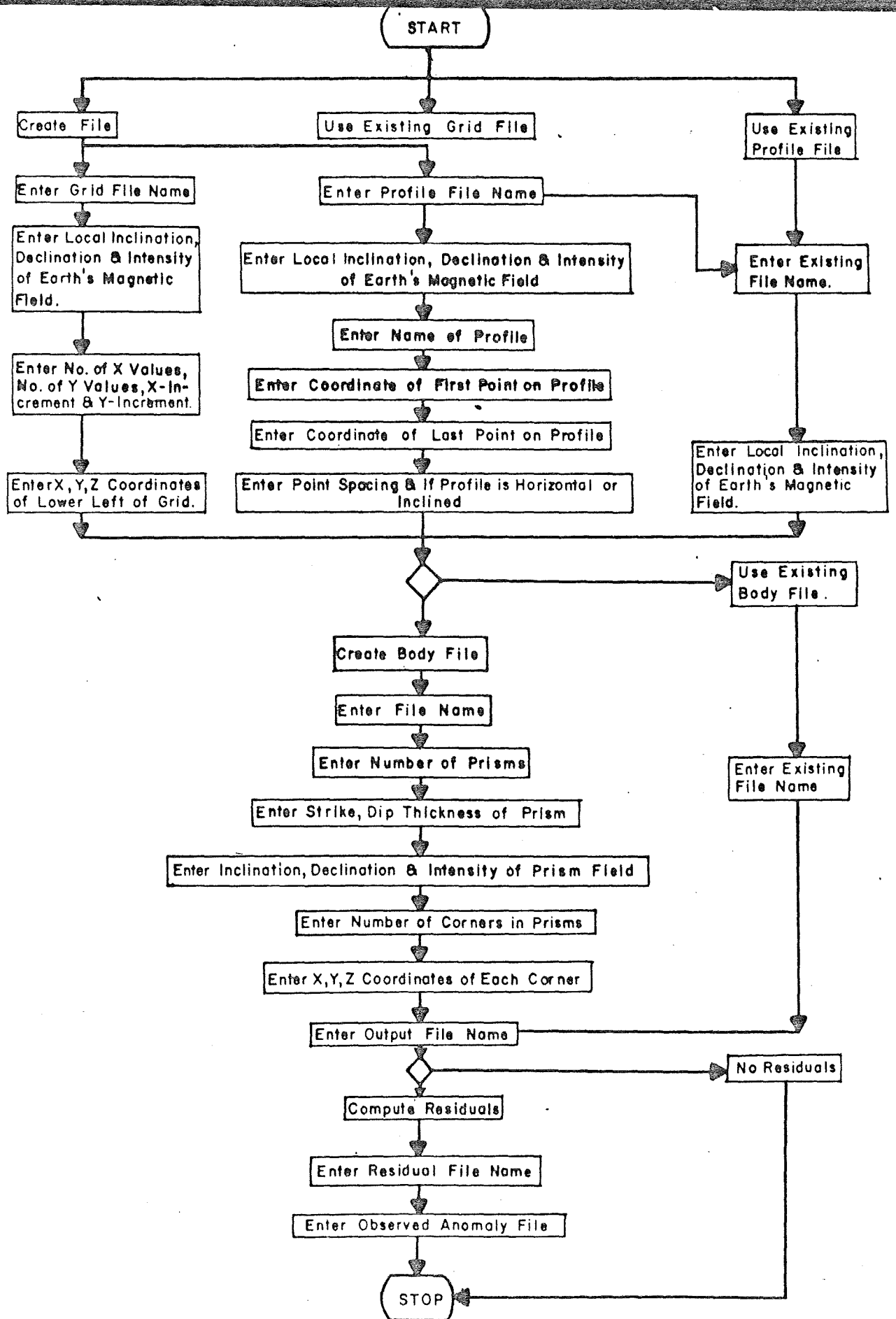


Figure 10. Generalized flow diagram for magnetic modelling computer program.

$J_{\text{NRM}}$  = intensity of natural remanent magnetization in the direction of the vector  $\vec{r}$ .

$\vec{J}$  = intensity of total magnetization.

Total magnetization of a lithologic unit can be calculated from measurements made on oriented rock samples. It can also be determined from the magnetic field measured over a body of rock if sufficient magnetic property contrasts exist and if the size and shape can be adequately constrained. The magnetizations determined by these two methods can differ considerably, because of vastly different sample sizes. A cored sample has a volume of approximately  $11 \text{ cm}^3$  while the volume of a rock unit used to determine total magnetization by matching the observed and calculated magnetic fields is typically 10 to  $100 \text{ km}^3$ .

The rock property information given in Table 1 shows total magnetization determined from cored samples and from matching magnetic fields. Measurements made by Grommé (personal communication) from 71 surface samples of Bishop Tuff yield a natural remanent magnetization ( $J_{\text{NRM}}$ ) of  $1070 \pm 590 \times 10^{-6} \text{ emu/cc}$ , a declination of  $355^\circ$  and inclination of  $55^\circ$ . Hoff (Pakiser and others, 1960) measured the susceptibility of Bishop Tuff as  $200 \times 10^{-6} \text{ emu/cc}$ . Using the above values for declination and inclination together with Gromme's greatest value of remanent magnetization ( $J_{\text{NRM}} = 1.430 \pm 370 \times 10^{-6} \text{ emu/cc}$ ) in the following expression, the total magnetization  $|J_{\text{T}}|$  is:

TABLE 1

## Comparison of Rock Magnetizations

Rock Unit	Intensity of total magnetization from the model <sup>(1)</sup>	Intensity of total magnetization from rock sample measurements <sup>(1)</sup>	$J_{NRM}$	$\theta^\circ$	$\sigma^\circ$	k	$I^\circ$	$D^\circ$
Bishop tuff	3200	1531	1430 <sup>(2)</sup>	55	355	200	62	17
altered Bishop tuff	300 to 700		160					
Wheeler Crest quartz monzonite	1750	309	226 <sup>(3)</sup>	58	345	165	62	17
Paleozoic metasediments	50 to 100	5	5 <sup>(3)</sup>	66	314	negligible		
Glass Mountain rhyolite	1550							
Round Valley Peak granodiorite	500 to 1000							
Mesozoic metavolcanics	200							

(1) all magnetizations are  $\times 10^{-6}$  emu/cc (2) measurements made by S. Gromme (3) measurements made by author

$\sigma$  = declination of  $J_{NRM}$

$I$  = inclination of local earth's field =  $62^\circ$

$\theta$  = inclination of  $J_{NRM}$

$D$  = declination of local earth's field =  $17^\circ E$

$J_{NRM}$  = natural remanent magnetization

$H$  = intensity of local earth's field = 51,900  $\gamma$

k = magnetic susceptibility

$$\begin{aligned}
 |J_T| &= \left[ (J_{\text{NRM}} \cos \theta \cos \sigma + kH \cos I \cos D)^2 \right. \\
 &\quad + (J_{\text{NRM}} \cos \theta \sin \sigma + kH \cos I \sin D)^2 \\
 &\quad \left. + (J_{\text{NRM}} \sin \theta + kH \sin I)^2 \right]^{\frac{1}{2}} \\
 &= 1531 \times 10^{-6} \text{ emu/cc.}
 \end{aligned}$$

(See Table 1 for explanation of units)

Considering the previously-discussed errors, the agreement is good. The higher total magnetization determined from matching magnetic fields suggests that the intracaldera Bishop Tuff is more densely welded than the tuff exposed in the Owen's River Gorge.

Measurements have been made on four samples of altered intracaldera Bishop Tuff. They have an average remanent magnetization of  $160 \times 10^{-6}$  emu/cc (Williams and others, 1977, p. 3037). The total magnetization from the model is 300 to  $700 \times 10^{-6}$  emu/cc.

The direction of magnetization for all but one of the rock units is taken to be coincident with the present earth's field direction in Long Valley. The natural remanent magnetization directions measured in this area (Table 1) tend to support this working hypothesis. The exception is the eastern half of the metavolcanic rocks which form the western third of the Mount Morrison roof pendant. These rocks are mostly the latite of Arrowhead Lake and the quartz latite tuff of Skelton Lake (Rinehart and Ross, 1964), and were modelled as having a reversed direction of magnetization. Possibly, some of this reversed direction of magnetization is a result of intense mechanical deformation as the bedding planes are nearly vertical.

RESULTS

The final prism magnetizations indicate that the magnetization of the Bishop Tuff in the western caldera has been substantially reduced. To calculate the final magnetic field, magnetizations for the unaltered Bishop Tuff in the eastern caldera and altered Bishop Tuff in the western caldera were taken to be  $3200 \times 10^{-6}$  and  $700 \times 10^{-6}$  emu/cc respectively. This reduction can be explained if the tuff in the western caldera is near its Curie temperature. A temperature of approximately  $500^{\circ}\text{C}$  would be required to produce the change in magnetization (Williams and others, 1977). However, there is no evidence that the tuff temperatures are so great. Geochemical thermometers indicate a reasonable minimum reservoir temperature of 200 to  $220^{\circ}\text{C}$  (Mariner and Willey, 1976). The most likely explanation for the reduced magnetization is hydrothermal alteration. Hydrothermal alteration is brought about by the interaction of hot magmatic emanations rich in water with the pre-existing solid rock. It includes chemical changes and changes resulting in the addition or removal of material by the circulating fluids. Much surface material is hydrothermally altered and the electrical investigations (Stanley and others, 1977) indicate extensive subsurface hydrothermal alteration is associated with the 1-to-10 ohm-m layer. Time, high temperature fluids and fracture porosity and permeability are required to significantly alter the magnetic mineralogy. The altered tuff located beneath the resurgent dome and between the Hilton Creek and Hartley Springs faults appears to have satisfied these requirements. Heat was periodically supplied from material vented to the surface during the resurgent episodes.

The altered and unaltered Bishop Tuff are abruptly separated by the Hilton Creek fault along its extension into the caldera. The steep magnetic gradients across this fault extension do not persist outside the caldera suggesting that it influences the movement of fluids through the fill in the western caldera. White (personal communication) suggested that the extent of alteration and the  $H_2S$  content of the fluids are also important if this process is to affect the magnetization.

There are indications that the alteration in the west part of the caldera may extend into the basement. Metasedimentary rocks of the Mount Morrison roof pendant are exposed outside the south ring fracture. Metasediments were encountered outside the northwest ring fracture during drilling in the Mono Craters tunnel (Putnam, 1949). This suggests that metasediments should be present beneath the fill in the western caldera basement. The magnetizations used when modelling these metasediments outside and inside the southern ring fracture are  $100 \times 10^{-6}$  and  $50 \times 10^{-6}$  emu/cc respectively. These indications of alteration are not as convincing as those for the tuff fill above.

The total volume of intracaldera Bishop Tuff in the final model is  $300 \text{ km}^3$ . Approximately 45 percent of this volume,  $135 \text{ km}^3$ , is hydrothermally altered. The final model contains  $77 \text{ km}^3$  of Glass Mountain rhyolite down-dropped inside the ring fracture. The combined volume of intracaldera Bishop Tuff and down-dropped Glass Mountain rhyolite is  $377 \text{ km}^3$ . Bailey and others (1976, p. 730) use a thickness of 1 km and the area of the subsided caldera block to estimate a volume of  $350 \text{ km}^3$  for the intracaldera Bishop Tuff. The estimate by Bailey and others for the volume of intracaldera Bishop Tuff is similar

to the combined volume of intracaldera Bishop Tuff and down-dropped Glass Mountain rhyolite determined from the magnetics. Muffler and Williams (1976) used the two refraction profiles to calculate a volume of  $450 \text{ km}^3$  for the intracaldera Bishop Tuff and down-dropped Glass Mountain rhyolite. The Muffler and Williams volume is  $73 \text{ km}^3$  greater than the volume estimated by the magnetic model.

There are several sources of error in these volume calculations. Some error in depth could occur in extending the refraction depths to areas between, and off to the sides of the two intersecting refraction lines. If the modelled magnetizations do not closely represent the effective magnetization of the real body over the volume being modelled, a significant volume error could occur. When the modelled magnetization is larger than the effective real magnetization, the modelled volume will be smaller than the real volume assuming that the real and model magnetic fields match. Indeed this error seems to have affected the volume of Bishop Tuff determined from the model. The magnetization determined from the model is about twice the magnetization determined from surface rock samples and the model volume is 86 percent of the volume determined by Bailey and others (1976). A more subtle error is caused by the variation of the magnetization along the boundary of the Bishop Tuff body. These variations can reduce to zero the magnetic contrast between the Bishop Tuff and adjacent rock units. In areas where this occurs some of the Bishop Tuff could be modelled as another rock unit.

In Figure 9, Stanley and others (1976) show that a conductive (1-10 ohm-m) zone which is 0.5 km thick lies above the basement rocks

inside the southeastern caldera. They interpret this zone as a high temperature reservoir in permeable volcanic rocks or as extensively hydrothermally altered rhyolitic tuffs. The magnetization assigned to the prisms in this area is  $350 \times 10^{-6} \text{ emu/cm}^3$  which is similar to the magnetization of the Round Valley Peak granodiorite and the Wheeler Crest quartz monzonite which are exposed just outside the southeast ring fracture. Two implications are possible: One, if the material in the conductive zone is Bishop Tuff, then its model magnetization suggests it is extremely altered. Second, the conductive zone may be material other than Bishop Tuff.

Two precaldera structures were identified beneath the fill. The identification is primarily based on the location and the magnetization of prisms in the model. Several prisms with a magnetization identical to that of Glass Mountain rhyolite are located beneath the Bishop Tuff in the northeast part of the caldera. These prisms extend from the Bishop Tuff to that segment of the outer ring fracture immediately adjacent to Glass Mountain. Their size, shape, location and magnetization produce the saddle which connects the magnetic high over the eastern caldera with the magnetic high over Glass Mountain. These prisms represent a part of Glass Mountain which was down-dropped into the caldera and covered with Bishop Tuff. The gravity model (Kane and others, 1976) shows a thick fill in this area. Possibly, the gravity anomaly is caused by a combination of Bishop Tuff and Glass Mountain rhyolite which both have low densities.

The second structure is located beneath the Bishop Tuff in the south central area of the caldera. Above this area the broad eastern magnetic high caused by the Bishop Tuff widens and merges with a small closed magnetic high (see A in Figure 5). The small, closed, magnetic high occurs over an outcrop of Round Valley Peak granodiorite which is located outside the caldera between Laurel Mountain and the south central ring fracture zone. In the model, a prism with a magnetization of  $500 \times 10^{-6}$  emu/cc is required to cause the broad magnetic high to widen and merge with the small magnetic high. This magnetization is the same as that used for prisms representing the Round Valley Peak granodiorite outside the caldera. The buried intracaldera prism is interpreted to be part of a precaldera mountain composed of Round Valley Peak granodiorite which has been down-dropped into the caldera (see B in Figure 5). The gravity model (Figure 3, Kane and others, 1976) shows less than 1.5 km of fill on top of this structure.

Several individual anomalies were examined. Two small closed magnetic lows are separated by the northeast ring fracture zone. The -257 gamma low (see C in Figure 5) lies over a volcanic vent exposed at 3,040 m (10,000 feet) on the northwest flank of Glass Mountain. This vent is both a gravity and magnetic low while the rest of Glass Mountain is a gravity and magnetic high. The most obvious explanation is that the material from this vent has reversed magnetic polarity. This is possible but another explanation is also attractive. No rocks with a reversed magnetic polarity have been found in the caldera. This magnetic low was modelled without using material which has a reversed magnetic polarity. The intensity of magnetization determined from the

model is  $1550 \times 10^{-6}$  emu/cc for the central section of Glass Mountain and is  $500 \times 10^{-6}$  emu/cc for the area surrounding the vent. The preferred explanation is that this vent contains low density material which is weakly magnetic relative to the material contained within the central portion of Glass Mountain.

Outside the caldera, the modelling results support the existence of several features inferred from the geology. The results suggest that the metamorphic rocks of the Mount Morrison roof pendant are at least 2.5 km (13,200 feet) thick and their contacts with the batholith granites are nearly vertical.

In conjunction with the modelling results, the magnetic high and gravity low over the Bald Mountain rhyodacite (Figure 2) suggests that the rhyodacite is generally a thin sheet. It seems to thicken near its northeast edge which could be the location of a source vent. Results suggest the rhyodacite pile which forms Mammoth Mountain (Figure 2) does not extend, except for a possible vent, below the topographic base of the Mountain which is at an elevation of about 2,710 m (9,000 feet). The modelling indicates that the quartz latite tuff of Skelton Lake (Figure 2) is either overturned or it has reversed magnetic polarity.

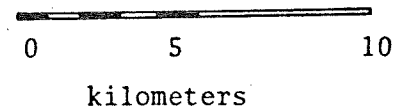
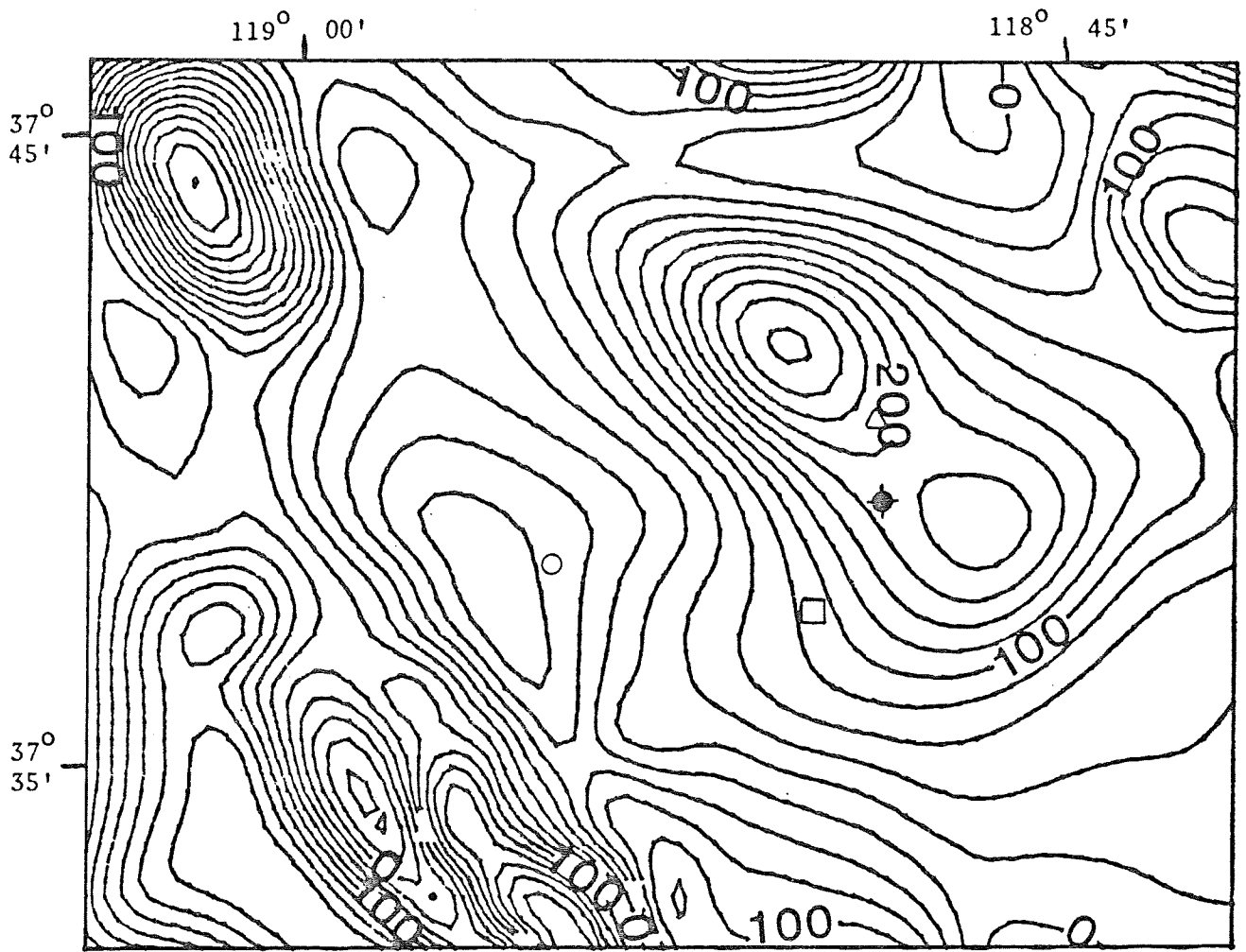
#### Discussion of the Residual Magnetic Field

The residual is calculated by subtracting the digital observed magnetic field from the digital calculated magnetic field. A residual is used as a measure of the accuracy with which the calculated magnetic field over the model (Figure 11) approximates the observed magnetic

field (Figure 12). A constant of 318 gammas is removed from each grid value of the residual. This produces a zero datum and makes it easier to see deviations of the calculated magnetic field from the observed magnetic field.

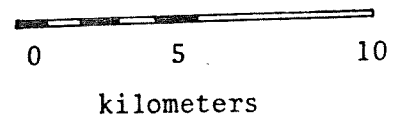
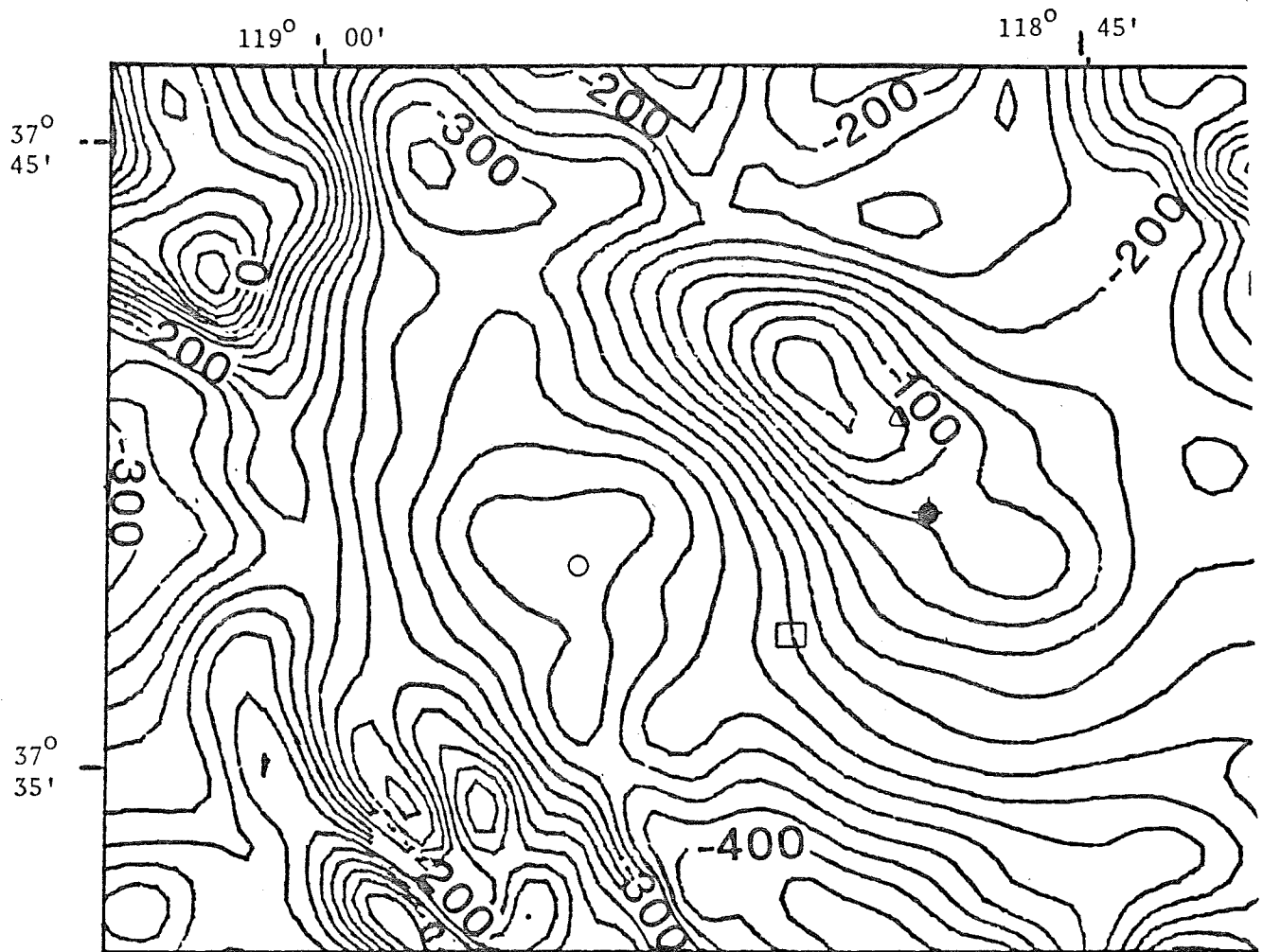
The residual (Figure 13) shows a pattern of low differences (good fit) over the caldera area and greater differences (poor fit) over the mountains surrounding the caldera. The stippled area between the 0 gamma contour and the +25 gamma contour represents 5 percent of the total magnetic relief (500 gammas) on the digitized aeromagnetic map. The intracaldera area with the poorest fit contains differences from -25 to -75 gammas.

This area extends in a northwest-southeast direction from the southwestern caldera across the western ring fracture zone to the edge of the map. Most contours on the residual map have this common northwest-southeast direction which suggests a common explanation. The contacts of the various metasedimentary, metavolcanic and intrusive rocks exposed in this part of the Sierra Nevada trend northwestward. These rocks are not well represented in the model.



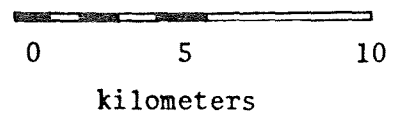
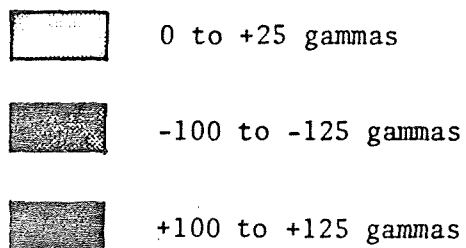
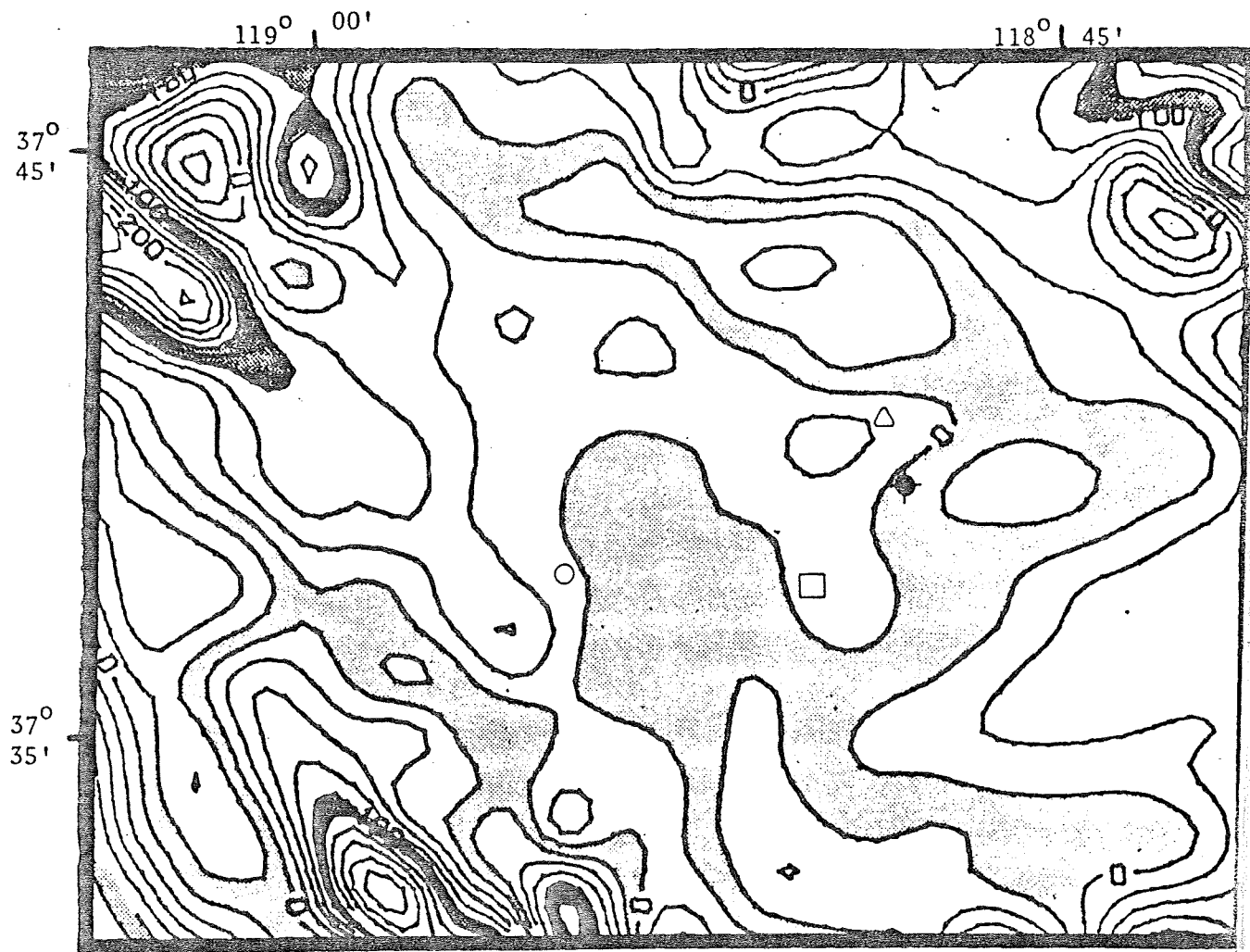
- △ Cashbaugh Ranch
- Whitmore Hot Springs
- Casa Diablo Hot Springs
- ◆ Republic Geothermal Well

Figure 11. Magnetic intensity map of Long Valley and vicinity calculated from the magnetic model.



- △ Cashbaugh Ranch
- Whitmore Hot Springs
- Casa Diablo Hot Springs
- ◆ Republic Geothermal Well

Figure 12. Digitized version of the high level magnetic intensity map of Long Valley and vicinity shown in Figure 5.



Contour interval 25 gammas

-  Cashbaugh Ranch
-  Whitmore Hot Springs
-  Casa Diablo Hot Springs
-  Republic Geothermal Well

Figure 13. Residual magnetic intensity map of Long Valley and vicinity (calculated magnetic field-observed magnetic field).

CONCLUSION

Aeromagnetic data were used to locate demagnetized zones within the Bishop Tuff; the demagnetization was probably caused by hydrothermal alteration. The most significant demagnetized zone is in the western caldera. Another demagnetized zone occurs along the south side of Hot Creek in the eastern caldera. The volume of altered Bishop Tuff in these zones as determined from the model is  $135 \text{ km}^3$  ( $32 \text{ mi}^3$ ). The total volume of Bishop Tuff in the caldera as determined from the model is  $300 \text{ km}^3$  ( $72 \text{ mi}^3$ ).

The exact location of a geothermal reservoir in Long Valley is little more than a guess. Fracture porosity probably increases between the intracaldera extensions of Hilton Creek and Hartley Springs faults. The heatflow data indicate a possible heat source beneath the western caldera (Lachenbruch and others, 1976). The most recent volcanism (Bailey and others, 1976) has occurred in the western caldera. The intensity and volume of alteration in the western caldera as derived from the magnetic data also suggest a reservoir there. The most likely location for a geothermal reservoir in Long Valley seems to be within the western caldera.

During 1976, Republic Geothermal drilled the "Long Valley #66-29" geothermal test well to a total depth of 2,109 m (6,920 feet) (Smith and Rex, 1977). The well location is shown on Figures 5, 12, 13 and 14. This well was drilled after the magnetic model study was completed. The well location was based primarily on the results of the electrical resistivity survey made by the U.S.G.S. (Stanley and others, 1976).

The Bishop Tuff was found at a depth of 696 m (2,285 feet); however, the well failed to penetrate the bottom of the Bishop Tuff. The maximum bottom hole temperature was 72°C. The model study predicted that the top and bottom of the Bishop Tuff would be encountered at 779 m (2,557 feet) and 2,730 m respectively.

This drilling information has at least two implications. First, the saddle between the two closed magnetic highs above the eastern half of the caldera is caused by altered Bishop Tuff rather than two separate accumulations of unaltered tuff. Second, the low bottom hole temperature suggests that the western caldera would be a more likely location for a geothermal reservoir in Long Valley.

REFERENCES CITED

- Bailey, R.A., 1973, Post-Subsidence Volcanism and Structure of Long Valley Caldera, California, Geol. Soc. Amer. Abstr. Programs 5 and 7.
- Bailey, R.A., Dalrymple, G.B. and Lanphere, M.A., 1976, Volcanism, Structure and Geochronology of Long Valley Caldera, Mono County, California, Jour. Geophys. Res., v. 81, n. 5, p. 725-744.
- Bateman, P.C., Clark, L.D., Huber, N.K., Moore, J.G., and Rinehart, C.D., 1963, The Sierra Nevada Batholith, A Synthesis of Recent Work Across the Central Part, U.S. Geol. Surv. Prof. Paper 414-D.
- Bateman, P.C. and Wahrhaftig, C., 1966, Geology of the Sierra Nevada, Geology of Northern California, Calif. Div. Mines Geol. Bull. 190, p. 107-172.
- Cain, J.C., Hendricks, S.J., Langel, R.A. and Hudson, W.V., 1967, A Proposed Model for the International Geomagnetic Reference Field-1965, Jour. Geomagnetism and Geoelectricity, v. 19, n. 4, p. 335-355.
- Christensen, M.N., 1966, Late Cenozoic Crustal Movements in the Sierra Nevada of California, Geol. Soc. Amer. Bull. 77, p. 163-182.
- Dalrymple, G.B., Cox, A. and Doell, R.R., 1965, Potassium-argon age and Paleomagnetism of the Bishop Tuff, California, Geol. Soc. Amer. Bull. 76, p. 665-674.
- Dalrymple, G.B., 1963, Potassium-argon dates of some Cenozoic Volcanic rocks of the Sierra Nevada, California, Geol. Soc. Amer. Bull., n. 74, p. 379-390.
- \_\_\_\_\_, 1964, Potassium-argon dates of three Pleistocene Interglacial basalt flows from the Sierra Nevada, California, Geol. Soc. Amer. Bull., n. 75, p. 753-757.
- Gilbert, C.M., 1938, Welded tuff in eastern California, Geol. Soc. Amer. Bull., n. 49, p. 1829-1862.
- Gilbert, C.M., Christensen, M.N., Al-Rawi, Yehya, and Lajoie, K.R., 1968, Structural and volcanic history of Mono Basin, California-Nevada in studies in Volcanology: Geol. Soc. Amer. Mem. 116, p. 275-329.
- Henderson, J.R., White, B.L. and others, 1963, Aeromagnetic map of Long Valley and Northern Owens Valley, California, U.S. Geol. Surv. Map GP-329.

- Plouff, Donald, 1975, Derivation of Formulas and FORTRAN Programs to Compute Magnetic Anomalies of Prisms: Nat'l. Tech. Info. Serv., No. PB-243-525, U.S. Dept. Commerce, Springfield, VA, 90 p.
- \_\_\_\_\_, 1976, Gravity and Magnetic Fields of Polygonal Prisms and Application to Magnetic Terrain Corrections, Geophys., v. 41, n. 4, p. 727-741.
- Rinehart, C.D. and Ross, D.C., 1957, Geology of the Casa Diablo Mountain Quadrangle, California, U.S. Geol. Surv. Geol. Quadrangle Map G9-99.
- \_\_\_\_\_, 1964, Geology and Mineral Deposits of the Mount Morrison Quadrangle, Sierra Nevada, California, U.S. Geol. Surv. Prof. Paper 385.
- Smith, J.L. and Rex, R.W., 1977, Drilling Results from the eastern Long Valley Caldera: in Energy and Mineral Resource Recovery (ANS TOPICAL MEETING, April 12-14, 1977), U.S.D.O.E., p. 529-540.
- Smith, R.S. and Bailey, R.A., 1968, Resurgent Cauldrons, Geol. Soc. Amer. Mem. 116, p. 613-662.
- Stanley, W.D., Jackson, D.B. and Zohdy, A.A.R., 1976, Deep Electrical Investigations in the Long Valley Geothermal Area, California, Jour. Geophys. Res., v. 81, n. 5, p. 810-820.
- Talwani, M., 1965, Computation with help of a Digital Computer of Magnetic Anomalies caused by Bodies of Arbitrary Shape, Geophys., v. 30, p. 797-817.
- U.S. Geological Survey, 1974, Aeromagnetic Map of parts of the Walker Lake and Mariposa 1° by 2° Quadrangles, eastern California, Open-File Report 74-109, U.S. Geol. Surv., Reston, VA.
- Williams, D.L., Berkman, F. and Mankinen, E.A., 1977, Implications of a Magnetic Model of the Long Valley Caldera, California, Jour. Geophys. Res., v. 82, n. 20, p. 3030-3038.